ChemPubSoc Europe

DOI: 10.1002/cptc.201900258

CHEMPHOTOCHEM Articles

Coumarin-4-ylmethyl- and *p*-Hydroxyphenacyl-Based Photoacid Generators with High Solubility in Aqueous Media: Synthesis, Stability and Photolysis

Karishma K. Adatia,[a] Thomas Halbritter,[b, e] Matiss Reinfelds,[b] Andre Michele,[a, c] Michael Tran,[a, c] Sabine Laschat,[c] Alexander Heckel,[b] Günter E. M. Tovar,*[a, d] and Alexander Southan*[a]

(Coumarin-4-yl)methyl (c4m) and *p*-hydroxyphenacyl (*p*HP)-based compounds are well known for their highly efficient photoreactions, but often show limited solubility in aqueous media. To circumvent this, we synthesized and characterized the two new c4m and *p*HP-based photoacid generators (PAGs), 7-[bis(carboxymethyl)amino]-4-(acetoxymethyl)coumarin (c4m-ac) and *p*-hydroxyphenacyl-2,5,8,11-tetraoxatridecan-13-oate (*p*HP-t), and determined their solubilities, stabilities and photolysis in aqueous media. The two compounds showed high solubilities in water of 2.77 mmol L^{-1} ± 0.07 mmol L^{-1} (c4m-ac) and 124.66 mmol L^{-1} ± 2.1 mmol L^{-1} (*p*HP-t). In basic conditions at pH 9, solubility increased for c4m-ac to 646.46 mmol L^{-1} ± 0.63 mmol L^{-1}, for *p*HP-t it decreased to 34.68 mmol L^{-1} ± 0.62 mmol L^{-1}. Photochemical properties of the two PAGs, such as the absorption maxima, the maximum molar absorption coefficients and the quantum yields, were found to be strongly pH-dependent. Both PAGs showed high stabilities $s_{24h} \geq 95\,\%$ in water for 24 h, but decreasing stability with increasing pH value due to hydrolysis. The present study contributes to a clearer insight into the synthesis, solubilities, stabilities, and photolysis of c4m and *p*HP-based PAGs for further photochemical applications when high PAG concentrations are required, such as in polymeric foaming.

1. Introduction

(Coumarin-4-yl)methyl (c4m) and *p*-hydroxyphenacyl (*p*HP)-based compounds are well known for their excellent photochemical properties such as their clean and highly efficient photo cleavage.[1] This was highlighted in an excellent review article by Givens *et al.*, who pointed out that c4m and *p*HP derivatives are especially well suited for time-resolved biochemical and physiological applications.[1a] Furthermore, these two chromophores are easy to access synthetically, can cover a wide range of excitation wavelengths from 250 nm to 450 nm by adjusting their substituents and can be used without sensitizer.[1a–c,e,2] Therefore, c4m and *p*HP-based compounds have gained considerable attention in biochemical,[1g,2e,3] agricultural[4] and pharmaceutical applications.[5] They have been used for neurotransmitter release,[5b] enzyme catalysis,[3a] membrane acidification,[6] or for drug delivery of anticancer agents.[7] Barman *et al.* for instance used *p*HP-benzothiazole-chlorambucil conjugates as a photoregulated drug delivery system due to its fast photocleavage and high biocompatibility.[5a] Moreover, c4m esters were employed to study proton migration in biological systems such as lipid bilayers.[6,8]

They were also used as photoacid generators (PAGs) to release acidic compounds under UV irradiation in aqueous media.[2a,b] However, in many water-based applications where high PAG concentrations are required, like in the field of bioinspired hydrogels,[9] hydrogel modifications[10] or foaming of polymeric materials,[11] strong electrolyte PAGs are preferred compared to weak electrolyte PAGs like c4ms or *p*HPs. For such applications, diphenyliodonium compounds are often used as strong electrolyte PAGs, which were discovered by Crivello *et al.* in 1977.[12] However, many diphenyliodonium-based PAGs like diphenyliodonium nitrate or diphenyliodonium antimonate are toxic, which significantly limits their application.[13] In fact, such PAGs cannot be implemented into biological, physiologi-

[a] K. K. Adatia, A. Michele, M. Tran, Prof. Dr. G. E. M. Tovar, Dr. A. Southan
Institute of Interfacial Process Engineering and Plasma Technology IGVP
University of Stuttgart
Nobelstr. 12, 70569 Stuttgart (Germany)
E-mail: alexander.southan@igvp.uni-stuttgart.de
guenter.tovar@igvp.uni-stuttgart.de
[b] Dr. T. Halbritter, Dr. M. Reinfelds, Prof. Dr. A. Heckel
Institute for Organic Chemistry and Chemical Biology
Goethe University Frankfurt
Max-von-Laue-Str. 7, 60438 Frankfurt/Main (Germany)
[c] A. Michele, M. Tran, Dr. S. Laschat
Institute of Organic Chemistry IOC
University of Stuttgart
Pfaffenwaldring 55, 70569 Stuttgart (Germany)
[d] Prof. Dr. G. E. M. Tovar
Fraunhofer Institute for Interfacial Engineering and Biotechnology IGB
Nobelstr. 12, 70569 Stuttgart (Germany)
[e] Dr. T. Halbritter
Department of Chemistry, University of Iceland, Dunhaga 3, 107 Reykjavik (Iceland)

Supporting information for this article is available on the WWW under https://doi.org/10.1002/cptc.201900258

cal and medical applications. Nevertheless, Gargava *et al.* used diphenyliodonium nitrate as PAG to regulate the pH-dependent pore size of bioinspired hydrogel valves.[9a] Also Feng *et al.* applied diphenyliodonium nitrate as PAG to trigger light controlled shape memory hydrogels.[10] The process involved shape retention through coordination interaction between the imidazole groups of the poly(acrylamide-co-*N*-vinylimidazole) hydrogel and dissolved metal ions in the aqueous swelling agent.[10] Shape recovery of the hydrogel was achieved by switching off the complexation *via* PAG photolysis reaction due to the protonation of imidazole groups.[10] Diphenyliodonium nitrate was also used to phototrigger the self assembly of a 1,3:2,4-dibenzylidene-D-sorbitol hydrogel in a controlled way when the pH was lowered.[9b] There are approaches to circumvent the toxicity of diphenyliodonium nitrate by using other photoacid generators like diaryliodonium tetrakis (pentafluorophenyl) borate or diphenyliodonium hexafluorophosphate, but they frequently need additional photosensitizers.[11] Kovalenko *et al.* for instance applied commercially available diaryliodonium tetrakis (pentafluorophenyl) borate (Silcolease UV Cata211) with low toxicity, but needed 2-isopropylthioxanthone as photosensitizer to tailor the porous structure of polydimethylsiloxane foams.[11b] A further example where strong electrolyte PAGs were favoured was published by Schlögl *et al.* for the foaming of 3D printed polyacrylate films.[11a] In particular, they utilized diphenyliodonium hexafluorophosphate as PAG and a toxic anthracene photosensitizer in combination with carbonate particles to generate CO_2 as foaming agent.[11a] The implementation of PAGs enabled them to simultaneously foam and cure their 3D printed polymers.[11a] Such 3D printed porous materials are subject to current research.[14] Especially in the above described fields of hydrogel research and polymeric foaming, c4m- and *p*HP-based PAGs could be beneficial, since they do not exhibit a cationic core structure which often limits biocompatibility. However, c4m- and *p*HP-based PAGs are rarely used, presumably due to the restricted or undetermined solubility of c4m and *p*HP-based PAGs in aqueous media. In some publications, a water solubility of c4m and *p*HP derivatives was reported,[1g,2b–d,15] but a solubility in aqueous media was not yet quantified, which is a crucial parameter for the PAG selection process.

Thus, to develop PAGs that would be usable in aqueous media in high concentration, we designed a c4m and a *p*HP derivative where a bis(carboxymethyl)amino moiety or a tri (ethylene glycol) moiety, respectively, should ensure high water solubility. The synthesis of 7-[bis(carboxymethyl)amino]-4-(acetoxymethyl)coumarin (c4m-ac) and *p*-hydroxyphenacyl-2,5,8,11-tetraoxatridecan-13-oate (*p*HP-t) (Scheme 1) is described and the solubility in aqueous media is quantified. We aimed to synthesize c4m and *p*HP-based PAGs with solubilities well above 1 mM in aqueous media, which are referred to as good in the c4m and *p*HP literature.[1g,2b–d,15] We furthermore characterized these new c4m and *p*HP-based PAGs and determined their photochemical properties, their pH dependent stability and photolysis in aqueous media. We envision that our studies will contribute to an increased applicability of c4m and *p*HP-based PAG in aqueous media, where high PAG concentrations are needed, like in hydrogel research or the field of polymeric foaming.

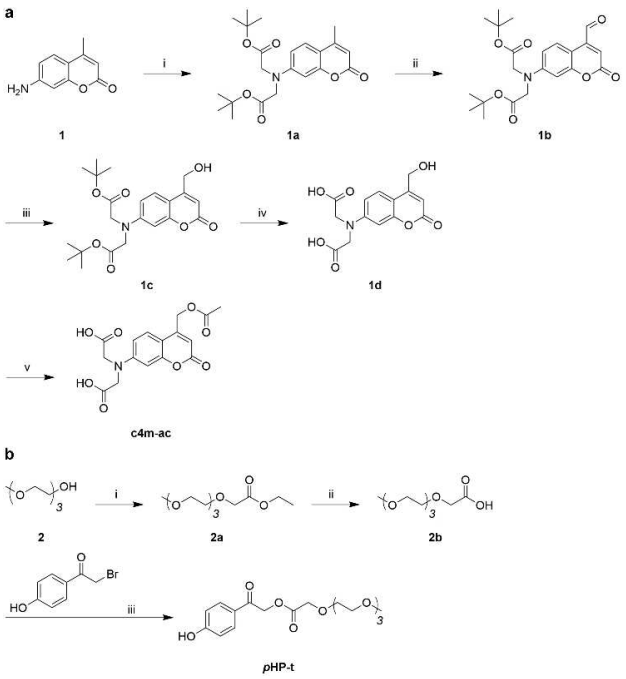

Scheme 1. Synthesis of a) 7-[bis(carboxymethyl)amino]-4-(acetoxy-methyl) coumarin (c4m-ac) over 5 steps with i) bromoacetic acid tert-butyl ester, NaI, ACN, 80 °C, 10 d, 43%; ii) SeO_2, *p*-xylene, 150 °C, 24 h, 80%; iii) $NaBH_4$, MeOH, RT, 2 h, 74%; iv) TFA, H_2O, CH_2Cl_2, RT, 25 min, 100%; v) 4-DMAP, EDC, AcOH, DMF, RT, 12 h, 63%. Synthesis of b) *p*-hydroxyphenacyl-2,5,8,11-tetraoxatridecan-13-oate (*p*HP-t) over 3 steps with i) NaH, bromoacetic acid ethyl ester, THF, RT, 3 h, 52%; ii) NaOH, MeOH, RT, 72 h, 86%; iii) NaOH, EtOH, 115 °C, 2 h, 49%.

2. Results and Discussion

2.1. Synthesis of c4m and *p*HP-based PAGs

The synthesis route and the molecular structures of the c4m and *p*HP-based PAGs, namely 7-[bis(carboxymethyl)amino]-4-(acetoxymethyl)coumarin (c4m-ac) and *p*-hydroxyphenacyl-2,5,8,11-tetraoxatridecan-13-oate (*p*HP-t), are shown in Scheme 1.

The synthesis of c4m-ac is based on previous work by Hagen *et al.* and started with the alkylation of 7-amino-4-methylcoumarin (**1**) with bromoacetic acid *tert*-butyl ester,[2c] followed by oxidation with SeO_2 to the corresponding aldehyde **1 b** which was subsequently reduced with $NaBH_4$ to the primary alcohol **1 c**. Deprotection of the carboxyl groups with trifluoroacetic acid yielded **1 d** which was acetylated with acetic acid in the presence of 4-dimethylaminopyridine (4-DMAP) and 1-ethyl-3-(3-dimethyl-aminopropyl) carbodiimide (EDC) to form c4m-ac. The ^1H NMR and ^{13}C NMR spectra of c4m-ac and its intermediates are given in Figures S1–5.

The synthesis of *p*HP-t was derived from Kaila *et al.*, whereby 3,6,9,12-tetraoxatridecanoic acid (**2 b**) was used as nucleophile instead of acetic acid (Scheme 1).[16] We used a

two-step synthesis to generate **2b** according to Le *et al. via* Williamson ether synthesis of tri(ethylene glycol) monomethyl ether (**2**) with ethyl bromoacetate and subsequent saponification reaction.[17] The nucleophilic substitution of 2-bromo-4-hydroxy-acetophenone with **2b** led to *p*HP-t. The ^{1}H NMR and ^{13}C NMR spectra of *p*HP-t and its intermediates are given in Figure S 6–8. Furthermore, *p*-hydroxyphenacylacetate (*p*HP-ac) was synthesized as reference substance according to Kaila *et al.* (Scheme S1).[16] Figure S9 shows the ^{1}H NMR and ^{13}C NMR spectra of *p*HP-ac.

Generally, all characterization data indicate that the syntheses yielded c4m-ac, *p*HP-t and *p*HP-ac in sufficient purity for further characterization as described below.

2.2. Solubility Determination

As the solubility of many c4m- and *p*HP-based derivatives were only estimated roughly in previous studies,[1g,2b–d,15] we wanted to quantify the solubilities $c_{max,w}$ and $c_{max,a}$ of c4m-ac and *p*HP-t in water and alkaline solution, respectively. Solubilities were determined photometrically by diluting saturated solutions of the compounds to diluted concentrations c_d. The value of c_d was determined by applying appropriate UV-vis calibrations for c4m-ac and *p*HP-t (Figure 1, Figure S10).[18] The solubilities $c_{max,w}$ and $c_{max,a}$ were then calculated with equation 2 (see Experimental Section) using the dilution factor.[19]

Figure 1 demonstrates the absorbance of c4m-ac and *p*HP-t at different concentrations as well as at c_d at the wavelength λ_{max} of maximum absorbance in water and basic medium. In water, λ_{max} of c4m-ac is at 366 nm and of *p*HP-t at 281 nm (Table 2). In alkaline solution, λ_{max} of c4m-ac shifts to 377 nm and of *p*HP-t to 327 nm (Table 2). Resulting values for c_d are listed Table S1 and $c_{max,w}$ and $c_{max,a}$ are shown in Table 1. c4m-ac shows a solubility $c_{max,w}$ in water of 2.77 mmol L^{-1} ± 0.07 mmol L^{-1} and a solubility $c_{max,a}$ in alkaline solution of 646.46 mmol L^{-1} ± 0.63 mmol L^{-1}. For *p*HP-t, a $c_{max,w}$ of 124.66 ± 2.19 mmol L^{-1} and a $c_{max,a}$ of 34.68 ± 0.62 mmol L^{-1} were found. Since PAG solubilities above 1 mmol L^{-1} in aqueous solutions were referred to as good,[2b,20] c4m-ac and *p*HP-t exhibit excellent solubility in water and basic solution. For comparison purposes, the solubilities of the reference substance *p*HP-ac were determined to be 14.40 ± 0.40 mmol L^{-1} ($c_{max,w}$) and 21.46 ± 8.58 mmol L^{-1} ($c_{max,a}$) (Figure S11).

In water, it becomes evident that the additional, hydrophilic tri(ethylene glycol) moiety present in *p*HP-t increased the solubility by a factor of 8.7 compared to *p*HP-ac, and thus the solubility enhancing effect of the tri(ethylene glycol) residue was clearly identified. In these conditions, the phenolic hydroxy

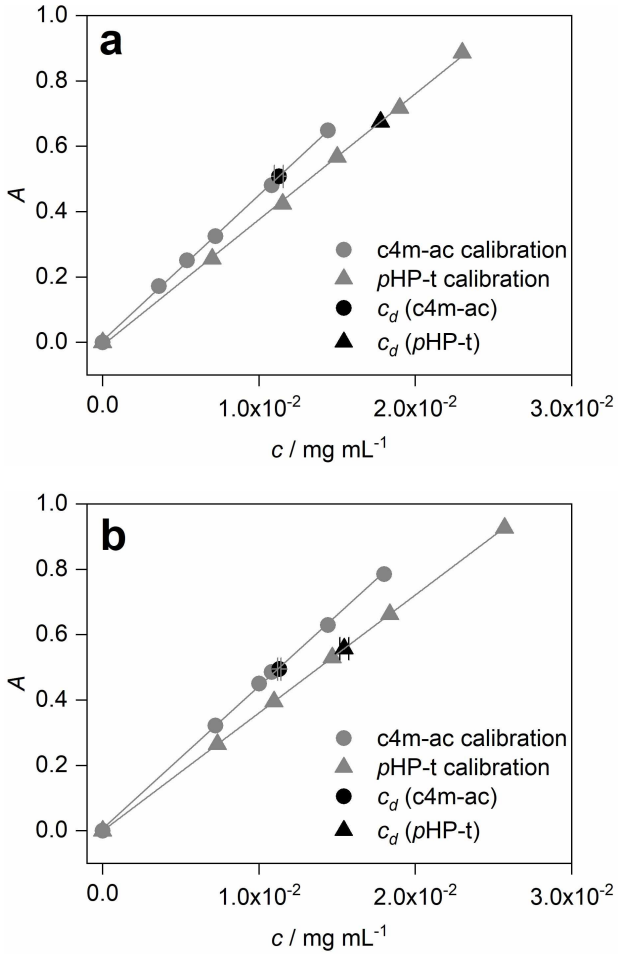

Figure 1. Absorbance A of c4m-ac and pHP-t solutions at different concentrations c for the photometric determination of the solubility in a) water and in b) alkaline solution at pH 9. The standard deviation of c_d is in the range of the symbol size.

Table 1. Solubility in water ($c_{max,w}$) and in alkaline solution ($c_{max,a}$) at pH 9 of the photoacid generators (PAGs) c4m-ac, *p*HP t and *p*HP-ac.

PAG	$c_{max,w}$ [mmol L^{-1}]	$c_{max,w}$ [g L^{-1}]	$c_{max,a}$ [mmol L^{-1}]	$c_{max,a}$ [g L^{-1}]
c4m-ac	2.77 ± 0.07	0.97 ± 0.02	646.46 ± 0.63	225.80 ± 0.22
*p*HP-t	124.66 ± 2.19	44.43 ± 0.78	34.68 ± 0.62	12.36 ± 0.02

Table 2. Wavelength λ_{max} at maximum absorption, molar absorption coefficient ε_{max} at λ_{max}, quantum yield Φ at the wavelength λ_{Φ} given in parentheses, molar absorption coefficients ε_{Φ} at λ_{Φ}. Tested solvents were water (w) and alkaline solution (a) at pH 9.

PAG	Solvent	λ_{max} [nm]	ε_{max} [L mol^{-1} cm^{-1}]	Φ (λ_{Φ})	ε_{Φ} [L mol^{-1} cm^{-1}]	$\Phi \cdot \varepsilon_{\Phi}$ [L mol^{-1} cm^{-1}]
c4m-ac	w	366	15 800	0.02 (365 nm)	15 800	320
c4m-ac	a	377	15 300	0.02 (365 nm)	13 900	280
*p*HP-t	w	281	13 500	0.69 (310 nm)	2 500	1700
*p*HP-t	a	327	12 900	0.07 (310 nm)	8 900	620
*p*HP-ac	w	281	11 600	0.46 (310 nm)	2 200	1000
*p*HP-ac	a	327	20 400	0.02 (310 nm)	15 300	300

group present in both *p*HP-t- and *p*HP-ac can be expected to be in its neutral form. Similarly, in c4m-ac the carboxylic acid groups will be partly protonated, resulting in a relatively low solubility in water.

In contrast, the solubility of c4m-ac in alkaline solution is boosted by a factor of 233 to the highest solubility observed in this study which can be explained by the more complete deprotonation of both carboxylic groups. A similar effect was observed for *p*HP-ac, however with only a moderate solubility increase by a factor of 1.5 due to the higher pK_a value of the phenolic hydroxy group compared to carboxylic acid groups. Interestingly, for *p*HP-t the solubility decreased in alkaline conditions although one could expect that also its phenolic group is deprotonated to a similar extent like in *p*HP-ac. We tend to explain this observation with a disruption of the hydrogen bonds between water and the tri(ethylene glycol) residue of *p*HP-t in salt-containing alkaline solution. Similar salting-out effects were reported by Brunchi *et al.*, who measured a decreasing solubility of poly(ethylene glycol) (PEG) in aqueous solution when adding electrolytes.[21] However, the solubility of *p*HP-t still was 1.6-fold higher in alkaline conditions than of *p*HP-ac.

Overall, *p*HP-t showed the highest solubility in water ($c_{max,w} = 124.66 \pm 2.19$ mmol L^{-1}) and c4m-ac demonstrated the highest solubility in basic solution ($c_{max,a} = 646.46$ mmol L$^{-1} \pm 0.63$ mmol L^{-1}) among the studied PAGs (Table 1).

2.3. Stability in Solution

As all PAGs investigated in this study contain at least one ester bond, hydrolysis may occur in aqueous solution. In order to quantify the influence of hydrolysis, the pH dependent stabilities *s* of c4m-ac, *p*HP-t and the reference compound *p*HP-ac in aqueous solution were investigated *via* HPLC. For this purpose, aqueous c4m-ac, *p*HP-t and *p*HP-ac solutions at pH 7, pH 8 and pH 9 were prepared and the PAG concentrations were measured after 1 h, 3 h, and 24 h storage time t_s under light exclusion at room temperature. Additionally, the stabilities of c4m-ac, *p*HP-t, and *p*HP-ac in water without pH adjustment after dissolution leading to pH 3, pH 6, and pH 5, respectively, were investigated. PAG stabilities were calculated according to equation 7. The resulting pH dependent stabilities are shown in Figure 2 (c4m-ac, *p*HP-t) and Figure S12 (*p*HP-ac) and are summarized in Table S2.

Generally, the studied PAGs showed high stabilities ($s_{24h} \geq 95\%$) for 24 h in slightly acidic solution as obtained without pH adjustment. At pH 7, c4m-ac showed the highest stability after 24 h ($s_{24h} = 99\%$), whereas *p*HP-t showed only limited stability ($s_{24h} = 85\%$) under the same conditions, compared to an s_{24h} value of 94% for *p*HP-ac. Upon increasing the pH value, stabilities generally decreased. At pH 8, c4m-ac still showed $s_{24h} \geq 95\%$, whereas for *p*HP-t s_{24h} dropped to 48% compared to an unaltered value of 94% for *p*HP-ac. At pH 9, all PAGs were significantly degraded with remaining concentrations of 11% (c4m-ac), 0% (*p*HP-t), and 53% (*p*HP-ac). Summarizing, the PAGs showed decreasing stability with increasing pH and time.

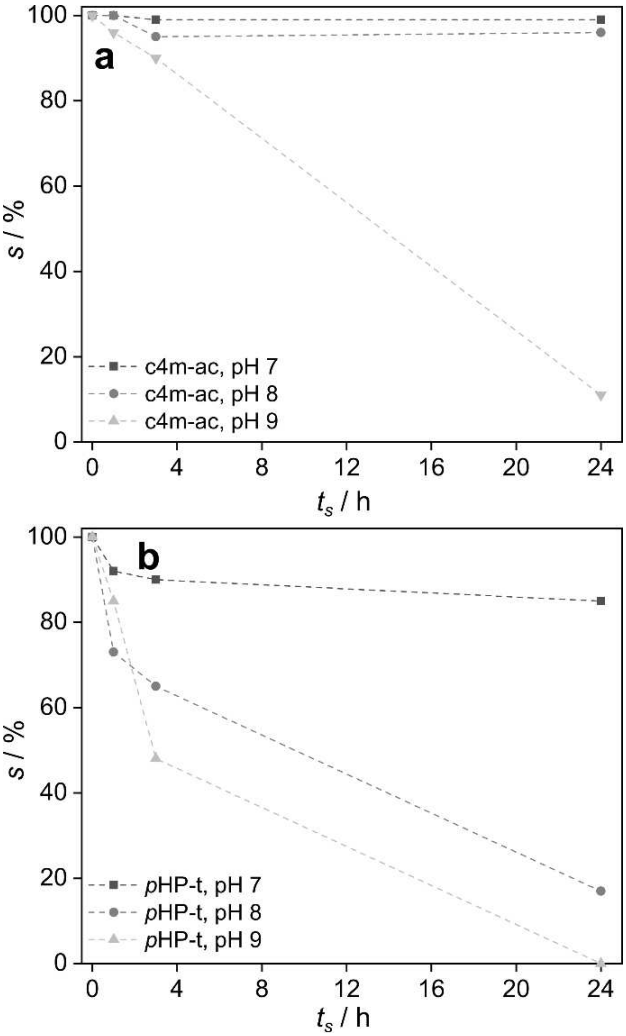

Figure 2. Stabilities *s* of the photoacid generators c4m-ac and pHP-t after a storage time t_s of 1 h, 3 h and 24 h at pH 7, pH 8 and pH 9. The stabilities were determined *via* HPLC and calculated according to Equation (7). The dashed lines are only for the guidance of the eye.

Because in all PAGs in this study, an ester bond is present, these observations can be ascribed to the faster ester bond hydrolysis under more alkaline conditions. For example, increasing hydrolysis rates were published for *p*HP-based esters at higher pH (>9), which is in line with our measurements (Table S2).[1a]

The results demonstrate that at neutral to moderately alkaline conditions (pH ≤ 8), c4m-ac is most resistant towards hydrolytic degradation. The stability of c4m-ac is in the range of other c4m-caged esters and amines from Hagen *et al.*, which are described to be highly resistant to spontaneous hydrolysis at pH 7.[2b] In contrast, Hagen *et al.* also reported hydrolysis of c4m-caged aryl alcohols, thioaryl alcohol and carbamates up to 10% at pH 7 during 24 h, which demonstrates the high stability of c4m-ac with less than 1% hydrolysis under comparable conditions.[2b,15]

As far as the stability of *p*HP derivatives is concerned, our results show that the leaving group present in the PAG influences its stability. At all pH values tested, *p*HP-t-showed

faster hydrolysis than *p*HP-ac. Rather fast hydrolysis of esters neighboring an oligo(ethylene glycol) moiety were reported before by Claaßen *et al.*[22] and can presumably be explained by the negative inductive effect of the tri(ethylene glycol) residue, resulting in a better carboxylate leaving group. The influence of the leaving group on *p*HP-based compounds can also be found in the literature: On the one hand, quantitative stabilities were reported for *p*HP esters and other *p*HP derivatives like *p*HP-adenosine triphosphate (ATP) in TRIS buffer at pH 7 after 24 h.[1g,23] On the other hand, *p*HP esters similar to *p*HP-t showed reduced stability.[2d,e] The di-alanine (Ala-Ala) *p*HP derivative *p*HP-Ala-Ala for instance hydrolyzed to 50% in TRIS buffer at pH 7 in less than 4 h.[2e]

In summary, hydrolysis is relevant for all PAGs studied, and has to be taken into account when considering to use these compounds in aqueous solution. Hydrolysis separates the acid from the chromophore, and therefore destroys the PAG functionality. Additionally, (unwanted) hydrolysis cannot be triggered and stopped as easily as (wanted) photolysis, and thus is a continuous process accompanying photolysis. Hence, PAG experiments, which are completed within a few minutes, can be performed at elevated pH values, but hydrolysis is certainly a disadvantage when solutions have to be stable for several hours. Therefore, photolysis conditions need to be chosen in such a way that hydrolysis plays only a minor role. For this reason, the photochemical properties of the PAGs are described in detail below.

2.4. Photochemical Properties

The reaction pathways for photolysis of c4m and *p*HP based compounds are well known as they were extensively investigated by Hagen *et al.* and Givens *et al.*, respectively.[1d,2b] Hagen *et al.* showed that c4m derivatives with the same coumarin group like in this study photolyse to 7-[bis (carboxymethyl) amino]-4-(hydroxymethyl)coumarin (c4m-OH) and the respective caged molecule.[2b] The photolysis of *p*HP derivatives in contrast is based on the Favorskii-rearrangement, which leads to *p*-hydroxy-phenylacetic acid and the corresponding caged compound, like acetic acid for *p*HP-ac.[1d] Both photoacid generation reactions of c4m and *p*HP based compounds are shown in Figure S17.

However, the efficiency of the photolysis reaction depends on the exact molecular structure and the solvent, which define the absorption coefficients and the quantum yields. Therefore, as a first step to assess the photochemical properties of c4m-ac and *p*HP-t as well as the reference compound *p*HP-ac, their UV-vis absorption spectra both in water as well as alkaline solution were measured directly after dissolution (Figure 3 and Figure S13). All studied PAGs contain acidic groups, so it can be expected that their absorption spectrum is pH dependent. In order to assess if this was the case, the wavelength λ_{max} at maximum absorption and the molar absorption coefficients ε_{max} at λ_{max} were extracted from the spectra (Table 2).

In water, the compound c4m-ac absorbed light up to 450 nm with a λ_{max} at 366 nm and an ε_{max} of 15800 L mol^{-1} cm^{-1}

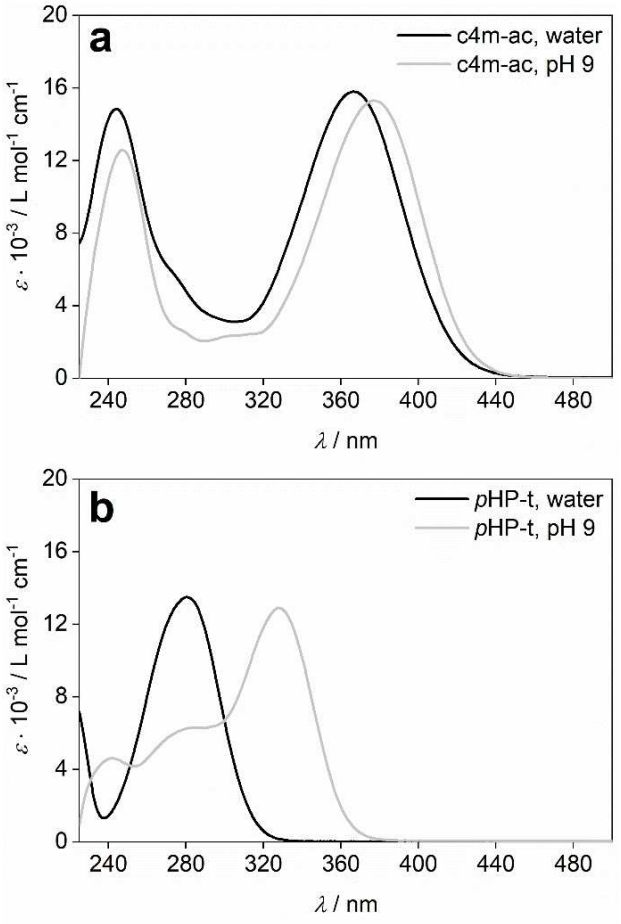

Figure 3. UV/Vis absorption spectra of a) c4m-ac and b) pHP-t in water and alkaline solution at pH 9.

(Table 2). This was in the range of other c4m-based compounds like c4m thioalcohol derivatives, which exhibited similar UV-vis absorption properties with λ_{max} between 376 nm and 383 nm as well as ε_{max} between 18300 L mol^{-1} cm^{-1} and 20000 L mol^{-1} cm^{-1} in hydroxyethyl piperazineethanesulfonic acid (HEPES) buffer at pH 7.[2b] In alkaline solution, the absorption band of c4m-ac shifted to longer wavelengths with a λ_{max} of 377 nm and an ε_{max} of 15300 L mol^{-1} cm^{-1}. This bathochromic shift was based on solvatochromic effects in alkaline solution, since the polarity of the alkaline solution was higher compared to water. Similar observations were reported from Liu and co-workers, who described a red shift of the UV-vis spectra of 7-aminocoumarins in more polar solvents.[24] Also Nad *et al.* published a λ_{max} shift of 7-amino-4-trifluoromethylcoumarin from 347 nm to 378 nm by increasing the solvent polarity from hexane to methanol.[25] Both explained that the higher the polarity of the solvent, the more intermolecular interactions between the coumarin moiety and the solvent can evolve, which stabilizes the ground state and shifts the UV-vis absorption to lower excitation energies.[24–25]

Compared to the two strong absorption bands of c4m-ac around 245 nm and 366 nm, *p*HP-t showed only one prominent π-π* absorption band from 240 nm to 320 nm with a λ_{max} at

281 nm and an ε_{max} of 13 500 L mol^{-1} cm^{-1} in water (Table 2). The λ_{max} of *p*HP-t shifted from 281 nm in water to 327 nm under basic conditions due to partly deprotonation of the phenol moiety. This phenoxide species contains an enlarged π-electron system, which leads to a bathochromic shift of the λ_{max} in alkaline solution. This is in accordance with multiple *p*HP derivatives published by Givens *et al.* who also reported a *p*K$_a$ value of 8.0 for *p*HP-ac.[2d] In alkaline conditions, the absorption spectrum of *p*HP-t therefore is a superposition of deprotonated and protonated *p*HP-t. In fact, between 250 nm and 300 nm the absorption of the remaining protonated form is still visible. Similar to c4m-ac, ε_{max} of *p*HP-t slightly decreased from 13 500 L mol^{-1} cm^{-1} in water to 12 900 L mol^{-1} cm^{-1} in alkaline solution (Table 2). For *p*HP derivatives this is quite unusual as most reported *p*HP phenoxide derivatives show significantly higher ε_{max} than their protonated counterparts.[2d] The measurements on *p*HP-ac with an ε_{max} of 11 600 L mol^{-1} cm^{-1} in water and an ε_{max} of 20 400 L mol^{-1} cm^{-1} in basic solution confirmed the trend in the literature (Figure S13, Table 2).[2d]

Apart from the molar absorption coefficients, quantum yields Φ are equally important in defining the rate of a photolysis reaction, as the rate is determined by the product of Φ and ε. Therefore, the photolysis quantum yields were measured at wavelengths near λ_{max}, *i.e.* 310 nm for *p*HP derivatives and 365 nm for c4m-ac (Table 2). For the photoacid generator photolysis, a high Φ value of 0.69 was found for *p*HP-t in water. In alkaline solution, Φ of *p*HP-t decreased to 0.07. Similarly, Φ of *p*HP-ac decreased from 0.46 in water to 0.02 in alkaline solution. The results for the two *p*HP-based compounds thus are in a similar range of other *p*HP-caged compounds with Φ values between 0.03 and 0.65 in water.[2d,26] Also the reduction of the quantum efficiency is in line with previous reports, where it was described that the conjugated phenoxide base has a much lower quantum yield than the protonated species.[2d,26a] This was attributed to a decreased intersystem crossing efficiency or competing nonproductive pathways.[2d,26a]

The Φ of c4m-ac in contrast was not influenced by the pH and stayed at a relatively low value of 0.02 in water and basic solution, as the two carboxylic acid groups of c4m-ac were not part of the conjugated π-electron system. The Φ values of c4m-ac were in the range of other c4m-caged compounds reported by Hagen *et al.* with Φ between 0.01 and 0.30 in ACN/HEPES-mixtures at pH 7.2.[2b,c]

A comparison of the different photolysis efficiencies is now possible by comparing the product of Φ and the molar absorption coefficient ε_{Φ} at the wavelength where the quantum yield was measured (Table 2). It becomes evident that the two *p*HP-based compounds showed higher photolysis rates than c4m-ac when irradiated during the quantum yield measurements. The fastest photoreaction was observed for *p*HP-t, which under such 'ideal' photolysis conditions is the most efficient PAG. The difference in photolysis rates could probably be further enhanced by irradiating closer to the respective λ_{max} values, assuming that the quantum yields at these wavelengths are similar to the measured ones.

2.5. Photolysis with a Broadband Light Source

The data on molar absorption coefficients and quantum yields in the previous section give insight into photolysis rates when using monochromatic light sources or light sources with a narrow emission spectrum such as lasers and LEDs. However, broadband light sources are common in non-photochemical laboratories when rather short irradiation wavelengths are needed like for the *p*HP based compounds. This is especially true in the fields of PAG application described in the introduction such as polymer chemistry, hydrogel curing, and 3D printing.[27] To evaluate which of the studied PAGs are favorable under such circumstances, we investigated the photolysis of c4m-ac, *p*HP-t, and *p*HP-ac at three different pH values using a standard broadband light source by HPLC (see Figure S16 for an exemplary HPLC dataset). The emission spectrum of the light source ranged between wavelengths of 300 nm and 450 nm (Figure SI15). The resulting PAG concentrations c against irradiation time t_{irr} of c4m-ac and *p*HP-t are shown in Figure 4, the respective data of the reference substance *p*HP-ac in Figure S14.

Generally, all PAGs disappeared completely during irradiation (Figure S16). The photolysis kinetics seem to follow a monoexponential decay of PAG concentrations. However, a correct physicochemical model describing the entire photolysis reaction will be more complex and the data were not fitted with a monoexponential function. Nevertheless, in order to compare the photolysis kinetics, the value of t_{irr}, which corresponds to a decrease of the concentration to half of the initial concentration, was determined. For c4m-ac, this was the case after 1 min to 2 min, for *p*HP-t after about 6 min, and for *p*HP-ac after about 15 min. These values were independent of the pH value of the solution. Interestingly, these results seem to contradict the results found in the previous sections because 1) *p*HP-t was previously identified to show the most efficient photolysis reaction, and 2) absorption spectra and/or quantum yields were found to depend on pH.

These findings can be explained by an interplay between the spectral overlap of the emission spectrum of the light source and the corresponding quantum yields. For c4m-ac, the absorption spectrum overlaps to a great extent with the lamp spectrum both in water as well as in alkaline conditions. Therefore, although the quantum yields were measured to be quite low, the photolysis proceeded rapidly in both conditions. In contrast, both *p*HP-t and *p*HP-ac absorption spectra in water overlap only to a minor extent with the lamp spectrum. Therefore, although quantum yields were measured to be much larger than for c4m-ac, photolysis was slower than for c4m-ac. The red shift of *p*HP-t and *p*HP-ac absorption spectra in alkaline conditions improves the overlap with the lamp spectrum, but concomitantly the quantum yields decreased drastically. These opposing effects obviously cancel each other out, so that no overall change of photolysis rates were observed upon changing the pH value.

In fact, the stable photolysis rates with various pH values simplify the usage of c4m-ac and *p*HP-t. This way, is possible to tune the pH value according to other experimental pre-

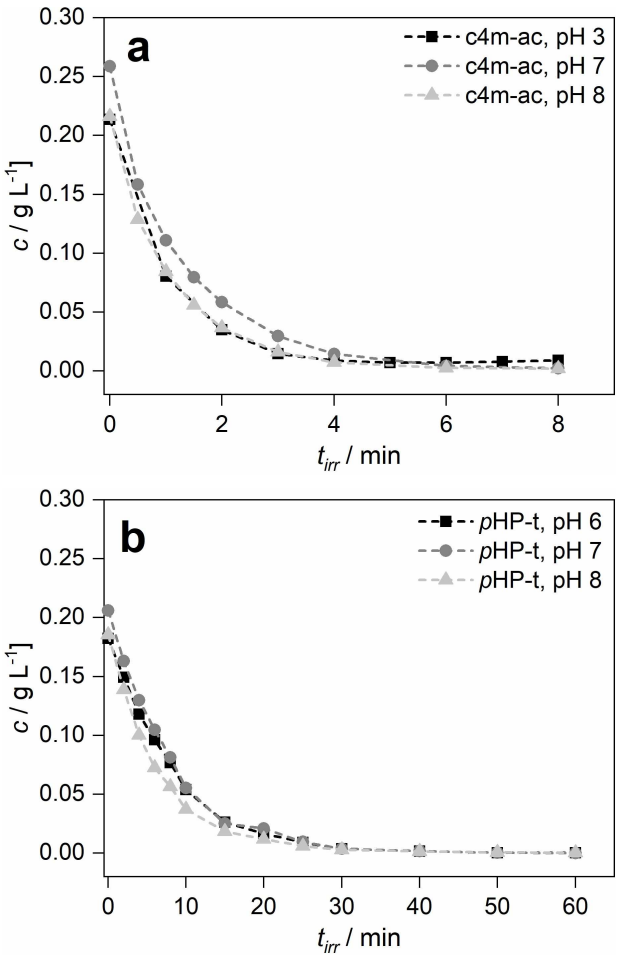

Figure 4. HPLC determined photolysis of c4m-ac and *p*HP-t in water, neutral (pH 7) and alkaline conditions (pH 8) during UV irradiation (300 nm–450 nm, ~40 mW cm^{-2}, UV light emission spectrum is given in Figure S15). For the photolysis measurements in water the pH was not adjusted, which lead to pH 3 for c4m-ac and to pH 6 for *p*HP-t at a concentration of c = 0.2 mg mL^{-1}. The photolysis is given by the decay of c during the irradiation time (t_{irr}). The lines are only for the guidance of the eye.

requisites without having to worry about the photolysis rate, given that the pH value is in a range where hydrolysis is not predominant. For prospective polymeric foaming experiments under these irradiation conditions, c4m-ac seems most advantageous compared to *p*HP-t due to the favorable absorption properties, the higher pH stability and the faster photolysis.

3. Conclusions

Our studies contribute to a comprehensive understanding of the synthesis, solubility, stability and photolysis of two highly water soluble c4m and *p*HP-based PAGs. This could help to satisfy the growing demand for water soluble PAGs especially in the field of hydrogel research and polymeric foaming. Yet, in such applications many strong electrolyte PAGs like diphenyliodonium salts are used, even if they are toxic or need additional sensitizer. This is mainly due to their good accessibility and high water solubility. With this work, we provided an alternative approach to such compounds by designing two easily accessible and highly water soluble c4m and *p*HP-based PAGs, as the substance classes of c4ms and *p*HPs are well suited for physiological applications and do not need additional sensitizers.[1a]

The successful synthesis of c4m-ac and *p*HP-t showed their accessibility and the introduction of the hydrophilic groups did not interfere with the excellent photochemical properties of c4m and *p*HP-based PAGs. We also investigated other key parameters like the stability and the photolysis of these PAGs, which confirmed that c4m-ac and *p*HP-t are fairly stable and well photo cleavable in aqueous media under varying pH conditions.

These properties should enable the use of c4m-ac and *p*HP-t for polymeric foaming, e.g. by using an alkaline carbonate solution and the *in situ* generated acid as foaming agent. We presume that c4m-ac and *p*HP-t are cytocompatible which would make them interesting candidates as PAGs *e.g.* for the production of 3D printed hydrogel foams as polymer scaffolds in tissue engineering. The question of cytocompatibility has to be addressed in future studies.

Experimental Section

Materials

2-Bromo-4-hydroxyacetophenone, 4-dimethylamino-pyridine (4-DMAP), 1-ethyl-3-(3-dimethylaminopropyl)-carbodiimide (EDC) and dichloromethane were purchased at TCI Germany GmbH (Eschborn, Germany). Ammonium chloride, hydrogen chloride, potassium permanganate, sodium hydride (60% dispersion in mineral oil), 7-amino-4-methylcoumarin, bromoacetic acid *tert*-butyl ester, sodium iodide, selenium dioxide, *p*-xylene, sodium borohydride, *N*,*N*-dimethylformamide (DMF) and sodium sulfate were obtained from Sigma-Aldrich Chemicals GmbH (Darmstadt, Germany). Ethyl bromoacetate was purchased from Alpha Aesar (Ward Hill, USA), sodium acetate (NaOAc) from Merck Chemicals GmbH (Darmstadt, Germany) and phenylalanine from Acros Organics (Geel, Belgium). Tri(ethylene glycol) monomethyl ether and sodium hydroxide were bought from Fluka Analytical (Munich, Germany). Diethylether and magnesium sulfate were purchased from AppliChem GmbH (Darmstadt, Germany). Acetic acid (AcOH), sodium chloride, sodium hydrogencarbonate and trifluoroacetic acid (TFA) were bought from Carl Roth GmbH + Co. KG (Karlsruhe, Germany). The solvents ethanol (EtOH), ethyl acetate (EtOAc), methanol (MeOH) and *n*-hexane were bought from VWR chemicals (Radnor, USA). Acetonitrile (MeCN) and tetrahydrofuran (THF) were obtained from J.T. Baker (Phillipsburg, USA). All chemicals and solvents were of the highest grade commercially available and were used without further purification. Thin-layer chromatography (TLC) analyses were performed on aluminum plates coated with silica gel 60 F 254 by Merck Chemicals GmbH (Darmstadt, Germany) and Nano-Silica gel RP-18 W by Fluka Analytical (Munich, Germany). For flash chromatography, silica gel 60 by Macherey-Nagel or silica gel 60 (0.063–0.200 mm) and LiChroprep RP-18 (40–63 μm) by Merck Chemicals GmbH (Darmstadt, Germany) were used. Water was purified with a TKA X-CAD Milli-Q system from Thermo Fischer Scientific (Waltham, USA).

Instrumentation

The NMR spectra of the c4m-based compounds were recorded on a Bruker AVIII-HD 500 MHz instrument from Bruker (Billerica, USA) equipped with a N_2 cooled cryogenic probe head using DMSO-d_6. The NMR spectra of the *p*HP-based compounds were recorded on a Bruker Avance 500 from Bruker (Billerica, USA) with $CDCl_3$ as solvent. Mass spectrometry was performed on an ESI-MS Bruker MicroTOFQ from Bruker (Billerica, USA) under nitrogen atmosphere.

For the measurement of the pH value an InLab 1 022 pH electrode from Mettler Toledo (Columbus, USA) in combination with a Lab 850 pH meter was used. Photolysis experiments were performed in an UV-H 255 UV chamber from Hartmann Feinwerkbau GmbH (Ober-Moerlen, Germany) with an irradiation intensity of approx. 40 mW cm^{-2} between 300 nm and 450 nm (Figure S15). The emission spectrum was determined with an Ocean Optics USB 2 000+ spectrometer from Ocean Optics Germany GmbH (Ostfildern, Germany). The distance between the bottom of the sample and the UV source in the UV chamber was 8.5 cm. UV-vis spectra were recorded in a two beam UV-vis spectrometer UV-2450 from Shimadzu (Kyoto, Japan) with quartz cuvettes of 1 cm path length and a cross-sectional area of 1 cm^2.

For quantum yield determinations c4m-ac was irradiated with a M365L2 LED from Thorlabs at 365 nm. For the irradiation of *p*HP-t and *p*HP-ac a M310L3 LED from Thorlabs (Newton, USA) at 310 nm was used. Both were operated by a DC4100 LED driver from Thorlabs (Newton, USA). The decay of c4m-ac was analyzed with a 1260 Infinity HPLC from Agilent Technologies Germany GmbH (Waldbronn, Germany), equipped with a diode array detector. Separation was done using MultoKrom® 100-5 C18 column (250× 4.6 mm) from CS-Chromatographie Service GmbH (Langerwehe, Germany). Chromatograms were analyzed with ChemStation software from Agilent Technologies Germany GmbH (Waldbronn, Germany).

For stability and photolysis determinations, HPLC measurements were performed using an analytical CBM-20A/20Alite HPLC from Shimadzu (Kyoto, Japan) with a Superspher 100 RP-18 (125 mm× 4.0 mm) column from Merck Chemicals GmbH (Darmstadt, Germany) and a SPD-M20A photodiode detector from Shimadzu (Kyoto, Japan). For c4m-ac a mixture of ACN:H_2O = 15%:85%, for *p*HP-t a mixture of ACN:H_2O = 17%:83% and for *p*HP-ac a mixture of ACN:H_2O = 10%:90% was used for elution. Trifluoroacetic acid (0.1%) was added to the HPLC solvent for *p*HP-t and *p*HP-ac. The flow rate was 1.0 mL min^{-1}. The HPLC chromatograms were analyzed with LCsolution software from Shimadzu (Kyoto, Japan).

Synthesis and Characterization

C4m-ac was synthesized by altering Hagen *et al.*'s synthesis route for c4m-based photoacid generators.[2c] *p*HP-t and the reference substance *p*-hydroxy-phenacyl acetate (*p*HP-ac) were synthesized by modifying the synthesis from Kaila *et al.* and Le *et al.*[16–17]

Di-*tert*-butyl 2,2′-((4-methyl-2-oxo-*2H*-chromen-7-yl)-azanediyl)diacetate (1 a)

7-Amino-4-methylcoumarin (**1**) (5.26 g, 30 mmol, 1.0 eq), bromoacetic acid *tert*-butyl ester (29.56 mL, 200 mmol, 6.7 eq), diisopropylethylamine (20.54 mL, 120 mmol, 4.0 eq) and NaI (4.5 g, 30 mmol, 1.0 eq) were dissolved in acetonitrile (90 mL) and stirred at 80 °C for 10 days. The mixture was cooled to room temperature (RT), filtered, and the solvent was removed under reduced pressure. The residue was dissolved in EtOAc (250 mL), washed with brine (3×50 mL), dried over Na_2SO_4 and the solvent was removed under reduced pressure. Purification *via* flash chromatography (silica, EtOAc:*n*-hexane = 1:4) afforded di-*tert*-butyl 2,2′-((4-methyl-2-oxo-2*H*-chromen-7-yl)azanediyl)diacetate (**1 a**) (5.08 g, 12.60 mmol, 42%) as a yellow oil. ^{1}H NMR (500 MHz, DMSO-d_6): δ [ppm] = 7.55 (d, *J* = 9.0 Hz, 1H), 6.57 (dd, *J* = 9.0 Hz, 2.5 Hz, 1H), 6.42 (d, *J* = 2.5 Hz, 1H), 6.03 (s, 1H), 4.18 (s, 4H), 2.50 (s, 3H), 1.42 (s, 18H). ^{13}C NMR (125 MHz, DMSO-d_6): δ [ppm] = 168.9, 160.5, 154.9, 153.5, 151.2, 126.0, 110.0, 109.1, 108.9, 98.0, 81.0, 53.5, 27.7, 17.9. ESI-MS (+): m/z: $[M+H]^+$ 404.19.

Di-*tert*-butyl 2,2′-((4-formyl-2-oxo-*2H*-chromen-7-yl)-azanediyl)diacetate (1 b)

Di-*tert*-butyl 2,2′-((4-methyl-2-oxo-*2H*-chromen-7-yl)azanediyl)diacetate (**1 a**) (4.03 g, 10 mmol, 1.0 eq) was dissolved in 50 mL *p*-xylene by heating, selenium dioxide (2.21 g, 20 mmol, 2.0 eq) was added, and the mixture was refluxed for 24 h. The mixture was filtered hot to remove black selenium, and the filtrate was concentrated under reduced pressure. The resulting precipitate afforded di-*tert*-butyl 2,2′-((4-formyl-2-oxo-*2H*-chromen-7-yl)azanediyl)diacetate (**1 b**) (3.41 g, 8 mmol, 80%) as orange-red powder. ^{1}H NMR (500 MHz, DMSO-d_6): δ [ppm] = 10.08 (s, 1H), 8.23 (d, *J* = 9.1 Hz, 1H), 6.76 (s, 1H), 6.64 (dd, *J* = 9.1 Hz, 2.6 Hz, 1H), 6.52 (d, *J* = 2.6 Hz, 1H), 4.21 (s, 4H), 1.42 (s, 18H). ^{13}C NMR (125 MHz, DMSO-d_6): δ [ppm] = 194.0, 168.7 160.9, 156.1, 151.5, 143.7, 126.4, 118.1, 109.8, 105.0, 98.4, 81.2, 53.5, 27.7. ESI-MS (+): m/z: $[M-H]^+$ 416.20.

Di-*tert*-butyl 2,2′-((4-(hydroxymethyl)-2-oxo-*2H*-chromen-7-yl) azanediyl)diacetate (1 c)

Di-*tert*-butyl 2,2′-((4-formyl-2-oxo-*2H*-chromen-7-yl)azanediyl)diacetate (**1 b**) (2.00 g, 5 mmol, 1.0 eq) was dissolved in MeOH (100 mL) and $NaBH_4$ (0.23 g, 6 mmol, 1.3 eq) was slowly added. The mixture was stirred at RT for 2 hours, diluted with H_2O (40 mL), acidified (pH 5) with 0.1 N HCl and extracted with CH_2Cl_2 (30 mL, 3×). The combined organic layers were washed with H_2O and brine, dried over Na_2SO_4 and the solvent was removed under reduced pressure. Purification by flash chromatography (hexane : EtOAc = 2:1) afforded di-*tert*-butyl 2,2′-((4-(hydroxymethyl)-2-oxo-*2H*-chromen-7-yl)azanediyl)diacetate (**1 c**) (1.6 g, 4 mmol, 74%) as yellow solid. ^{1}H NMR (500 MHz, DMSO-d_6): δ [ppm] = 7.48 (d, *J* = 9.0 Hz, 1H), 6.54 (dd, *J* = 9.0 Hz, 2.6 Hz, 1H), 6.43 (d, *J* = 2.6 Hz, 1H), 6.15 (t, *J* = 1.4 Hz, 1H), 5.54 (t, *J* = 10 Hz, 1H), 4.68 (d, *J* = 3.0 Hz, 2H), 4.18 (s, 4H), 1.42 (s, 18H). ^{13}C NMR (125 MHz, DMSO-d_6): δ [ppm] = 168.9, 160.9, 156.8, 154.9, 151.1, 124.9, 108.9, 107.4, 105.3, 98.1, 81.1, 59.0, 53.5, 27.7. ESI-MS (+): m/z: $[M+H]^+$ 420.19.

2,2′-((4-(Hydroxymethyl)-2-oxo-*2H*-chromen-7-yl)azanediyl) diacetic acid (1 d)

Di-*tert*-butyl 2,2′-((4-(hydroxymethyl)-2-oxo-2*H*-chromen-7-yl)azanediyl)diacetate (**1 c**) (0.50 g, 1 mmol) was stirred in a mixture of TFA/H_2O/CH_2Cl_2 (74:1:25) (20 mL) at RT for 25 min. The solvent was removed under reduced pressure and coevaporated with Et_2O (2×), dissolved in a acetonitrile-water mixture, lyophilized and afforded 2,2′-((4-(hydroxymethyl)-2-oxo-*2H*-chromen-7-yl)azanediyl) diacetic acid (**1 d**) (0.37 g,1 mmol) quantitatively. ^{1}H NMR (500 MHz, DMSO-d_6): δ [ppm] = 7.47 (d, *J* = 9.0 Hz, 1H), 6.56 (dd, *J* = 9.0, 2.6 Hz, 1H), 6.45 (d, *J* = 2.6 Hz, 1H), 6.14 (t, *J* = 1.4 Hz, 1H), 4.68 (d, *J* = 1.0 Hz, 2H), 4.21 (s, 4H). ^{13}C NMR (125 MHz, DMSO-d_6): δ [ppm] = 171.4, 160.9, 156.8, 154.9, 151.1, 125.0, 108.9, 107.3, 105.2, 98.0, 59.0, 52.8. ESI-MS (+): m/z: $[M+H]^+$ 308.15.

7-[bis(carboxymethyl)amino]-4-(acetoxymethyl)coumarin (c4m-ac)

2,2′-((4-(Hydroxymethyl)-2-oxo-*2H*-chromen-7-yl)azanediyl)diacetic acid (**1 d**) (0.10 g, 0.3 mmol, 1.0 eq), 4-DMAP (0.12 g, 1 mmol, 3.0 eq), EDC (0.17 g, 1 mmol, 3.0 eq) and AcOH (51 µL, 1 mmol, 3.0 eq) were dissolved in DMF (5 mL) and stirred at RT for 12 hours. The solvent was removed under reduced pressure. Purification *via* RP-HPLC afforded 7-[bis(carboxymethyl)amino]-4-(acetoxymethyl)coumarin (0.07 g, 0.2 mmol, 63 %) (c4m-ac) as yellow solid. ^{1}H NMR (500 MHz, DMSO-d_6): δ [ppm] = 12.85 (s, 2H), 7.51 (d, J = 9.0 Hz, 1H), 6.60 (dd, J = 9.0 Hz, 2.3 Hz, 1H), 6.48 (d, J = 2.3 Hz, 1H), 6.10 (s, 1H), 5.28 (s, 2H), 4.23 (s, 4H), 2.16 (s, 3H). ^{13}C NMR (125 MHz, DMSO-d_6): δ [ppm] = 171.4, 170.0, 160.4, 155.1, 151.5, 150.6, 125.4, 109.2, 106.9, 106.6, 98.1, 61.1, 52.8, 20.5. ESI-MS (+): m/z: $[M+H]^+$ 350.13.

Ethyl-2,5,8,11-tetraoxatridecan-13-oate (2 a)

Under nitrogen atmosphere tri(ethylene glycol) monomethyl ether (**2**) (5.54 g, 34 mmol, 1.0 eq) and sodium hydride (1.62 g, 67 mmol, 2.0 eq) were dissolved in anhydrous THF (100 mL) at 0 °C. Ethyl bromoacetate (14.09 g, 84 mmol, 2.5 eq) was added at RT, stirred for two hours and filtrated. The white residue was dissolved in NH_4Cl solution at 0 °C and the aqueous phase was extracted with EtOAc. The combined organic phases were washed with water and dried over $MgSO_4$. The solvent and the excess of ethyl bromoacetate were removed under reduced pressure to afford ethyl-2,5,8,11-tetraoxatridecan-13-oate (**2 a**) (4.37 g, 17 mmol, 52 %) as a colorless oil. ^{1}H-NMR (500 MHz, $CDCl_3$): δ [ppm] = 4.22 (q, J = 7.2 Hz, 2H), 4.15 (s, 2H), 3.64-3.75 (m, 10H), 3.54-3.56 (m, 2H), 3.38 (s, 3H), 1.29 (t, J = 6.9 Hz, 3H). ^{13}C NMR (125 MHz, $CDCl_3$): δ [ppm] = 170.5, 71.9, 70.9-70.6, 68.7, 60.8, 59.0, 14.2. ESI-MS (+): m/z: $[M+Na]^+$ 273.13 Da.

2,5,8,11-Tetraoxatridecan-13-oic acid (2 b)

The ester **2 a** (0.98 g, 4 mmol, 1.0 eq) was dissolved in a 1 M methanolic solution of sodium hydroxide (22.00 mL, 20 mmol, 5.0 eq) and stirred for 72 hours at RT. The solution was adjusted to a pH value of 3 by adding aqueous HCl solution. The solvent was removed under reduced pressure and the residue was dissolved in diethylether. Unsoluble solid was separated through filtration and the organic phase was washed with water. By evaporating the solvents 2,5,8,11-tetraoxatridecan-13-oic acid (**2 b**) (0.75 g, 3 mmol, 86 %) could be obtained as colorless oil. ^{1}H NMR (500 MHz, $CDCl_3$): δ [ppm] = 8.33 (s, 1H), 4.17 (s, 2H), 3.77-3.75 (m, 2H) 3.70–3.64 (m, 8H), 3.59–3.57 (m, 2H), 3.39 (s, 3H). ^{13}C NMR (125 MHz, $CDCl_3$): δ [ppm] = 172.8, 71.9–70.32, 68.9, 58.9. ESI-MS (−): m/z: $[M-H]^-$ 221.1 Da.

p-hydroxyphenacyl-2,5,8,11-tetraoxatridecan-13-oate (*p*HP-t)

2,5,8,11-tetraoxatridecan-13-oic acid (**2 b**) (0.76 g, 3 mmol, 2.0 eq) were added to a 0.5 M aqueous sodium hydroxide solution (4.2 mL, 2 mmol, 1.1 eq) and stirred at RT for 10 minutes. 2-Brom-4-hydroxyacetophenone (0.36 g, 2 mmol, 1.0 eq) were dissolved in EtOH (15 mL) and heated under reflux conditions for 2 hours. After removing the solvent under reduced pressure the oily residue was dissolved in water and adjusted to a pH 8 by adding saturated sodium hydrogencarbonate solution (3.5 mL). The aqueous phases were extracted with dichloromethane and the combined organic phases were washed with brine and dried over sodium sulfate. The solvent was evaporated under reduced pressure and the raw product was purified *via* column chromatography (silica, *n*-hexane : EtOAc = 1 : 2, EtOAc, EtOAC : MeOH = 1 : 9). The solvent was removed under reduced pressure to afford *p*-hydroxyphenacyl-2,5,8,11-tetraoxatridecan-13-oate (*p*HP-t) (0.29 g, (1 mmol, 49 %) as colorless oil. ^{1}H NMR (500 MHz, $CDCl_3$): δ [ppm] = 7.80 (dt, J = 8.8 Hz, 2.7 Hz, 2H), 6.91 (dt, J = 8.8 Hz, 2.7 Hz, 2H), 5.32 (s, 2H), 4.30 (s, 2H), 3.76–3.75 (m, 2H), 3.70–3.64 (m, 8H), 3.57–3.55 (m, 2H), 3.37 (s, 3H). ^{13}C NMR (125 MHz, $CDCl_3$): δ [ppm] = 190.3, 170.2, 161.6, 130.4, 126.6, 115.8, 71.9, 70.9–70.4, 68.5, 66.1, 59.0. ESI-MS (−): m/z: $[M-H]^-$ 355.15 Da.

p-hydroxyphenacylacetate (*p*HP-ac)

2-Bromo-4-hydroxyacetophenone (1.48 g, 7 mmol, 1.0 eq) were dissolved in EtOH and a mixture of sodium acetate (1.12 g, 8 mmol, 1.2 eq) and AcOH (0.36 mL, 6 mmol, 0.9 eq) in water (3.6 mL) was added dropwise. The solution was heated for 3 h at 90 °C under reflux conditions. The solvent was removed under reduced pressure and the remaining oily residue was dissolved in aqueous sodium carbonate solution. The aqueous phase was extracted with EtOAc and the combined organic phases were washed with brine and dried over sodium sulfate. After evaporation of the solvent, the raw product was recrystallized from EtOAc and purified by a column chromatography (*n*-hexane : EtOAc = 7 : 3). *p*-hydroxyphenacylacetate (*p*HP-ac) (0.97 g, 5 mmol, 73 %) was obtained as a white solid. ^{1}H NMR (500 MHz, $CDCl_3$): δ [ppm] = 7.83 (dt, J = 8.8 Hz, 2.8 Hz, 2H), 6.89 (dt, J = 8.8 Hz, 2.8 Hz, 2H), 6.19 (s, 1H), 5.30 (s, 2H), 2.24 (s, 3H). ^{13}C-NMR (125 MHz, $CDCl_3$): δ [ppm] = 190.8, 170.9, 160.9, 130.4, 127.1, 115.7, 65.8, 20.7. ESI-MS (−): m/z: $[M-H]^-$ 193.03 Da.

Solubility Determination

The solubilities of c4m-ac, *p*HP-t and *p*HP-ac were determined photometrically in water and alkaline solution (3 M $KHCO_3$ solution, pH 9).[18] For the determination of the solubility in water ($c_{max,w}$) and the solubility in alkaline solution ($c_{max,a}$) a calibration curve was prepared by measuring the UV-vis absorption spectra of the PAGs at four different concentrations in water and in basic solution (Figure S10).

The concentrations were selected in such a way that the absorbance maxima were spread over the linear absorbance range (A_λ = 0.1–0.9) of the Beer's law [Eq. (1)].[28]

$$A_\lambda = \varepsilon_\lambda c d \quad (1)$$

In this equation, A_λ is the absorbance at a specific wavelength λ, ε_λ is the molar absorption coefficient at the wavelength λ, c is the concentration and d is the path length. The calibration curve was used to determine the molar absorption coefficient ε_λ of the PAG in the respective media. Three saturated PAG solutions were prepared and diluted until the absorbance maxima were in the linear absorbance range. To calculate the concentration of the diluted sample (c_d) the previously determined molar absorption coefficient ε_λ was used. As shown in Equation (2), the solubility in water $c_{max,w}$ can be quantified by multiplying the concentration of the diluted PAG solution c_d with the dilution factor d_f.

$$c_{max,w} = \frac{A_\lambda}{\varepsilon_\lambda \cdot d} \cdot d_f = c_d \cdot d_f \quad (2)$$

The solubility in alkaline solution $c_{max,a}$ is determined respectively by using A_λ, ε_λ and d_f of the alkaline solution. The solubility determination was performed in triplicates.

Quantum Yield Determination

All measurements were performed in 1 cm quartz fluorescence cuvette from Hellma GmbH (Müllheim, Germany). For irradiation of c4m-ac, a M365 L2 LED from Thorlabs at 365 nm was used and for *p*HP-t and *p*HP-ac, an M310L3 LED from Thorlabs (Newton, USA) at 310 nm was applied. Both were operated by a DC4100 LED driver from Thorlabs (Newton, USA). Light sources were calibrated using iron (III) ferrioxalate actinometry, following the literature procedure.[29] The photo reaction of c4m-ac was followed by HPLC and of *p*HP-t and *p*HP-ac by UV-vis spectroscopy. All quantum yields (Φ) were measured in triplicates and calculated as previously described.[30]

For the Φ determination of c4m-ac, an aqueous sample of c4m-ac containing the internal standard phenylalanine was irradiated at 365 nm and the conversion was analyzed *via* HPLC. The conversion change (in %) of c4m-ac was plotted against irradiation time (t_{irr}). The plot was fitted using following exponential decay function [Eq. (3)], where A_1 and t_1 are fit parameters and y_0 is a constant.[30]

$$y = A_1 e^{\frac{t_{irr}}{t_1}} + y_0 \tag{3}$$

The initial rate of the concentration change (y') at the beginning of the irradiation can be calculated by deriving Equation (3) and inserting the corresponding fit parameters for $t_{irr} = 0$ [Eq. (4)]:[30]

$$y' = -\frac{A_1 e^{\frac{-t_{irr}}{t_1}}}{t_1} \tag{4}$$

For c4m-ac, Φ is then calculated by Equation (5), where c is the concentration of the irradiated solution, V is the volume of the irradiated sample, y' is the change in concentration, n_p is the photon flux of the light source determined by actinometry and A_λ is the absorbance of the PAG solution at the irradiation wavelength.[30]

$$\Phi = \frac{c \cdot V \cdot y'}{n_p \cdot (1 - 10^{-A_\lambda})} \tag{5}$$

In contrast to c4m-ac, Φ of *p*HP-t and *p*HP-ac was determined by UV-vis spectroscopy. Therefore, *p*HP-t and *p*HP-ac samples with a high absorption ($A_\lambda > 3$) at 310 nm were used to ensure complete absorption of radiant flux. The *p*HP-based PAGs were irradiated and the change of absorption was measured simultaneously using a photodiode array detector. A plot of the absorption change against irradiation time was prepared choosing a suitable wavelength with $A_\lambda < 1$. The decrease of the absorption in the initial phase of the reaction (conversion $< 10\,\%$) was fitted by a linear regression. Φ of *p*HP-t and *p*HP-ac was calculated using Equation (6):

$$\Phi = \frac{-k\ V}{d \cdot \varepsilon_\lambda \cdot\ n_p} \tag{6}$$

Here, k is the slope from the linear regression, V is the volume of the irradiated sample, d is the pathlength of the cuvette, ε_λ is the molar absorption coefficient of the wavelength used for the reaction control (here at 321 nm) and n_p is the photon flux of the light source.

Stability Determination

C4m-ac, *p*HP-t and *p*HP-ac were dissolved in water at a concentration of 0.2 g L^{-1}, which led to pH 3 for c4m-ac, pH 6 for *p*HP-t and pH 5 for *p*HP-ac. Aliquots of these PAG solutions were adjusted to pH 7 and pH 8 with 0.01 M NaOH. The samples were stored under light exclusion at RT for 1 h, 3 h and 24 h. After filtration, they were measured *via* HPLC. The elution time (t_{elu}) of c4m-ac was 6.3 min, of *p*HP-t 9.0 min and of *p*HP-ac 9.5 min. The PAG stability (s) was calculated according to Equation (7), where $P_{t=0}$ is the peak area of the PAG immediately after preparation ($t = 0$) and P_t is the respective peak area after a storage time t_s.

$$s = \frac{P_t}{P_{t=0}} \tag{7}$$

Photolysis

An aqueous solution of c4m-ac, *p*HP-t and *p*HP-ac was prepared with a concentration of 0.2 mg mL^{-1}. This led to a solution of pH 3 for c4m-ac, of pH 6 for *p*HP-t and of pH 5 for *p*HP-ac, respectively. An aliquot of each PAG solution was adjusted to pH 7 and to pH 8 using 0.01 M NaOH. 1 mL samples of the PAG solutions were irradiated in a quartz glass cuvette using a hartmann.gs UV-H 255 UV chamber. The irradiation time t_{irr} was adjusted to the photolysis speed of the compound. The photolysis of c4m-ac for instance was measured after 0.5 min, 1 min, 1.5 min, 2 min, 3 min, 4 min, 6 min and 8 min UV irradiation. For *p*HP-t, the photolysis was measured every two minutes for the first 10 minutes and then every 5 minutes. After 30 min, *p*HP-t was analyzed every 10 minutes until an overall t_{irr} of 60 minutes. For *p*HP-ac, the concentration was measured every minute in the first 10 minutes and afterwards every five minutes up to 80 minutes.

Acknowledgements

K. A. gratefully acknowledges financial support by the Evonik Foundation. We thank the University of Stuttgart and the Fraunhofer-Gesellschaft for provision of infrastructure and gratefully acknowledge generous financial support by the Carl Zeiss Foundation and the University of Stuttgart within the Projekthaus NanoBioMater. The contribution by A.H. was made possible by SFB 902 and GRK 1986 of the Deutsche Forschungsgemeinschaft.

Conflict of Interest

The authors declare no conflict of interest.

Keywords: coumarin-4-ylmethyl · photoacid generators · *p*-hydroxyphenacyl · photolysis · stability · water solubility

[1] a) R. S. Givens, M. Rubina, J. Wirz, *Photochem. Photobiol. Sci.* **2012**, *11*, 472–488; b) X. Du, H. Frei, S.-H. Kim, *Biopolymers* **2001**, *62*, 147–149; c) P. Klán, T. Šolomek, C. G. Bochet, A. Blanc, R. Givens, M. Rubina, V. Popik, A. Kostikov, J. Wirz, *Chem. Rev.* **2013**, *113*, 119–191; d) R. S. Givens, D. Heger, B. Hellrung, Y. Kamdzhilov, M. Mac, P. G. Conrad, E. Cope, J. I. Lee, J. F. Mata-Segreda, R. L. Schowen, J. Wirz, *J. Am. Chem.*

Soc **2008**, *130*, 3307–3309; e) R. Schmidt, D. Geissler, V. Hagen, J. Bendig, *J. Phys. Chem.* **2005**, *109*, 5000–5004; f) R. S. Givens, B. Matuszewski, *J. Am. Chem. Soc* **1984**, *106*, 6860–6861; g) R. S. Givens, C.-H. Park, *Tetrahedron Lett.* **1996**, *37*, 6259–6262.

[2] a) A. P. Pelliccioli, J. Wirz, *Photochem. Photobiol. Sci.* **2002**, *1*, 441–458; b) V. Hagen, B. Dekowski, N. Kotzur, R. Lechler, B. Wiesner, B. Briand, M. Beyermann, *Chem. Eur. J.* **2008**, *14*, 1621–1627; c) V. Hagen, B. Dekowski, V. Nache, R. Schmidt, D. Geißler, D. Lorenz, J. Eichhorst, S. Keller, H. Kaneko, K. Benndorf, *Angew. Chem. Int. Ed.* **2005**, *44*, 7887–7891; d) R. S. Givens, K. Stensrud, P. G. Conrad, A. L. Yousef, C. Perera, S. N. Senadheera, D. Heger, J. Wirz, *Can. J. Chem.* **2011**, *89*, 364–384; e) R. S. Givens, J. F. W. Weber, P. G. Conrad, G. Orosz, S. L. Donahue, S. A. Thayer, *J. Am. Chem. Soc* **2000**, *122*, 2687–2697; f) V. R. Shembekar, Y. Chen, B. K. Carpenter, G. P. Hess, *Biochemistry* **2007**, *46*, 5479–5484.

[3] a) S. Geibel, A. Barth, S. Amslinger, A. H. Jung, C. Burzik, R. J. Clarke, R. S. Givens, K. Fendler, *Biophys. J.* **2000**, *79*, 1346–1357; b) T. Ohtsuki, S. Kanzaki, S. Nishimura, Y. Kunihiro, M. Sisido, K. Watanabe, *Nat. Commun.* **2016**, *7*, 12501; c) Y. Hotta, T. Kaneko, R. Hayashi, A. Yamamoto, S. Morimoto, J. Chiba, T. Tomohiro, *Chem. Asian J.* **2019**, *14*, 398–402.

[4] a) S. Atta, A. Jana, R. Ananthakirshnan, P. S. Narayana Dhuleep, *J. Agric. Food Chem.* **2010**, *58*, 11844–11851; b) S. Atta, M. Ikbal, A. Kumar, N. D. Pradeep Singh, *J. Photochem. Photobiol.* **2012**, *111*, 39–49.

[5] a) S. Barman, S. K. Mukhopadhyay, S. Biswas, S. Nandi, M. Gangopadhyay, S. Dey, A. Anoop, N. D. Pradeep Singh, *Angew. Chem. Int. Ed.* **2016**, *55*, 4194–4198; b) K. Kandler, L. C. Katz, J. A. Kauer, *Nat. neurosci.* **1998**, *1*, 119; c) T. Buckup, A. Southan, H.-C. Kim, N. Hampp, M. Motzkus, *J. Photochem. Photobiol.* **2010**, *210*, 188–192.

[6] D. Geißler, Y. N. Antonenko, R. Schmidt, S. Keller, O. O. Krylova, B. Wiesner, J. Bendig, P. Pohl, V. Hagen, *Angew. Chem. Int. Ed.* **2005**, *44*, 1195–1198.

[7] L. H. Al-Wahaibi, H. M. Abu-Melha, D. A. Ibrahim, *J. Chem.* **2018**, *2018*, 8.

[8] S. Serowy, S. M. Saparov, Y. N. Antonenko, W. Kozlovsky, V. Hagen, P. Pohl, *Biophys. J.* **2003**, *84*, 1031–1037.

[9] a) A. Gargava, C. Arya, S. R. Raghavan, *ACS Appl. Mater. Interfaces* **2016**, *8*, 18430–18438; b) D. J. Cornwell, O. J. Daubney, D. K. Smith, *J. Am. Chem. Soc* **2015**, *137*, 15486–15492.

[10] W. Feng, W. Zhou, S. Zhang, Y. Fan, A. Yasin, H. Yang, *RSC Adv.* **2015**, *5*, 81784–81789.

[11] a) S. Schlögl, M. Reischl, V. Ribitsch, W. Kern, *Prog. Org. Coat.* **2012**, *73*, 54–61; b) A. Kovalenko, K. Zimny, B. Mascaro, T. Brunet, O. Mondain-Monval, *Soft matter* **2016**, *12*, 5154–5163.

[12] J. V. Crivello, J. H. W. Lam, *Macromolecules* **1977**, *10*, 1307–1315.

[13] M. Shirai, M. Tsunooka, *Prog. Polym. Sci.* **1996**, *21*, 1–45.

[14] a) F. Schuster, T. Hirth, A. Weber, *J. Appl. Polym. Sci.* **2019**, *136*, 46977; b) R. Kankala, F.-J. Lu, C.-G. Liu, S.-S. Zhang, A.-Z. Chen, S.-B. Wang, *Materials* **2018**, *11*, 1390; c) F. Schuster, F. N. Ngamgoue, T. Goetz, T. Hirth, A. Weber, M. Bach, *J. Mater. Chem. C* **2017**, *5*, 6738–6744.

[15] V. Hagen, F. Kilic, J. Schaal, B. Dekowski, R. Schmidt, N. Kotzur, *J. Org. Chem.* **2010**, *75*, 2790–2797.

[16] N. Kaila, K. Janz, S. DeBernardo, P. W. Bedard, R. T. Camphausen, S. Tam, D. H. H. Tsao, J. C. Keith, C. Nickerson-Nutter, A. Shilling, R. Young-Sciame, Q. Wang, *J. Med. Chem.* **2007**, *50*, 21–39.

[17] a) H. T. Le, B. N. Hong, Y. R. Lee, J. H. Cheon, T. H. Kang, T. W. Kim, *Bioorg. Med. Chem. Lett.* **2016**, *26*, 699–705; b) A. Williamson, *Philos. Mag.* **1850**, *37*, 350–356.

[18] R. Panchadhayee, A. K. Misra, *ARKIVOC* **2009**, 298–307.

[19] A. D. McNaught, A. Wilkinson, **1997**, *Blackwell Scientific Publications,*, Oxford.

[20] D. A. Pella, *University of Minnesota* **2012**.

[21] C.-E. Brunchi, L. Ghimici, *Rev. Roum. Chim.* **2013**, *58*, 183–188.

[22] C. Claaßen, M. H. Claaßen, F. Gohl, G. E. M. Tovar, K. Borchers, A. Southan, *Macromol. Biosci.* **2018**, *18*, 1800104.

[23] C.-H. Park, R. S. Givens, *J. Am. Chem. Soc* **1997**, *119*, 2453–2463.

[24] X. Liu, J. M. Cole, K. S. Low, *J. Phys. Chem. C.* **2013**, *117*, 14731–14741.

[25] S. Nad, H. Pal, *J. Phys. Chem. A.* **2001**, *105*, 1097–1106.

[26] a) K. Zou, W. T. Miller, R. S. Givens, H. Bayley, *Angew. Chem. Int. Ed.* **2001**, *40*, 3049–3051; b) K. Zou, S. Cheley, R. S. Givens, H. Bayley, *J. Am. Chem. Soc* **2002**, *124*, 8220–8229; c) R. S. Givens, J.-I. Lee, *J. Photosci.* **2003**, *10*, 37–48.

[27] a) K. K. Adatia, S. Keller, T. Götz, G. E. M. Tovar, A. Southan, *Polym. Chem.* **2019**, 4485–4494; b) A. Hiller, K. Borchers, G. E. M. Tovar, A. Southan, *Addit. Manuf.* **2017**, *18*, 136–144.

[28] A. Beer, *Ann. Physik* **1852**, *162*, 78–88.

[29] C. Hatchard, C. A. Parker, *Proc. R. Soc. Lond. A Math. Phys. Sci.* **1956**, *235*, 518–536.

[30] M. Reinfelds, J. von Cosel, K. Falahati, C. Hamerla, T. Slanina, I. Burghardt, A. Heckel, *Chem. Eur. J.* **2018**, *24*, 13026–13035.

Manuscript received: October 29, 2019
Revised manuscript received: December 12, 2019
Accepted manuscript online: December 16, 2019
Version of record online: January 16, 2020